

# Investigation of Toxicity Properties of Flower-like ZnO Nanoparticles on *Cyprinus carpio* Sperm Cells Using Computer-Assisted Sperm Analysis (CASA)

Mustafa Erkan Ozgur<sup>1</sup>, Ahmet Ulu<sup>2</sup>, Sevgi Balcioglu<sup>2</sup>, Imren Ozcan<sup>2</sup>, Fatih Okumuş<sup>3</sup>, Suleyman Koytepe<sup>2</sup>, Burhan Ates<sup>2</sup>

<sup>1</sup>Inonu University, Fishery Faculty, Department of Aquaculture, 44280, Malatya, TURKEY

<sup>2</sup>Inonu University, Science Faculty, Department of Chemistry, 44280, Malatya, TURKEY

<sup>3</sup>Inonu University, Sürgü Vocational High School, Department of Computer Technology, 44280, Malatya, TURKEY

Phone: +904225216742

Email: mustafa.ozgur@inonu.edu.tr

## Abstract

This study was carried out to clarify the toxicity properties of Flower-like *zinc oxide* nanoparticles (ZnO NPs) on collected sperm samples from *Cyprinus carpio* using computer-assisted sperm analysis (CASA). Flower-like ZnO NPs were successfully synthesized using a simple system at 120°C for 5 h by the microwave-assisted solvothermal techniques. The synthesized ZnO NPs were characterized for its structural, morphological and thermal properties. After that, the different concentrations of synthesized ZnO NPs (0.001, 0.01, 0.1, 0.5, 1 ppm) were examined with *Cyprinus carpio* sperm samples collected from Karakaya reservoir. The spermatozoa motility parameters which contain to curvilinear velocity (VCL), straight line velocity (VSL), average path velocity (VAP), straightness (STR), amplitude of lateral head displacement (ALH), and beat cross frequency (BCF) was computed and recorded by CASA. According to the results, while VCL, VAP and BCF were statistically significant ( $P < 0.05$ ), VSL, ALH and STR were not statistically significant ( $P > 0.05$ ). In addition, the EC50 values of VCL and VAP parameters were calculated 0.56 ppm and 0.004 ppm, respectively.

**Key words:** *Cyprinus carpio*, ZnO nanoparticles, Spermatozoa motility, CASA, Toxicity

## Introduction

Along with increasing pollution in the aquatic environment, the monitoring of the toxicity of the pollutants, understanding of its mechanism and determination of the available effective areas are necessary for environmental risk assessment. The studies which determining the ineffective maximum concentration level of environmental contaminant on fertility are not enough. *In vitro* techniques provide valuable methods for applying a wide range of concentrations and exposure times to compare toxicity levels of environmental contaminant, and for studying mechanisms and sites of action (Hatef, Alavi, Golshan, & Linhart, 2013). Unlike mammals, the sperms of the teleost fish start to move immediately after they have come into contact with water, and these movements take only a few minutes. On the other hand, their motility can be maintained with partial dilution using some diluents for 24 h and water can improve spermatozoa motility again. To monitor sublethal effects of pollutants on the production system, toxicity test can be conducted incubating for 24 h with pollutants in the diluter as well as exposed to contaminants during final dilution (Kime et al., 1996).<sup>[E1]</sup> So, the toxicity test of sperm *in vitro* can be conducted directly or through incubation with pollutant.<sup>[ÖME2]</sup>

In common carp, spermatozoa cells are the most primitive among teleost fishes and have very short spermatogenesis period. The annual spermatozoa production in this fish species is about 190 billion/kg per fish

weight. Their spermatozoa cells have not any acrosome as other teleost fish. The size of spermatozoa head (include nucleus) is 2.5-3  $\mu\text{m}$ , length of spermatozoa tail, 40  $\mu\text{m}$ . After spermatogenesis, sperm has stocked in testicles and to ready spawning in the spring following that same year (Billard, Cosson, Percec, & Linhart, 1995). The spermatozoa of teleost fishes (especially in marine fish species) are completely immotile until they encounter the outer aquatic environment or the female fish ovarium fluid. Nonetheless, the changes in pH of sperm channel during the last maturation can trigger spermatozoa motility to a certain degree (Coward, Bromage, Hibbitt, & Parrington, 2002). In common carp, the motility of common carp spermatozoa can be started by the pH values of outside between 6-9. Therefore, spermatozoa motility is significantly affected by intracellular and extracellular pH values in the starting and duration of mobility of the sperm cell. Furthermore, spermatozoa activity of most teleost fishes having external fertilization strategy tends to decrease during motility period. For example, the duration of motility is very short, 20-25 seconds in trout, 1-2 minutes in common carp (Alavi & Cosson, 2005). Also, the fertilizing ability of spermatozoa rapidly declines due to following initiation of motility, due to the sudden decrease in motility and velocity due to depletion of ATP content and the change in morphological features involved in motility, such as permeability of the plasma membrane (Alavi et al., 2012; Billard, Cosson, Percec, & Linhart, 1995; Hatef, Alavi, Golshan, & Linhart, 2013). Computer-assisted sperm analysis systems (CASA) are a very important method for the practical analysis in many numbers of spermatozoa motility, and the system is used in place of estimation methods based on subjective opinion of the individual emotional of the analyst as well as classical methods used in the past. The CASA can determine the many motility parameters of sperm cells such as VSL: straight line velocity ( $\mu\text{m/s}$ ), VCL: curvilinear velocity ( $\mu\text{m/s}$ ), VAP: angular path velocity ( $\mu\text{m/s}$ ), used to track the route STR: straightness of average route, BCF: beat cross frequency (cross/second), ALH: amplitude of lateral displacement of the spermatozoa head ( $\mu\text{m}$ ) and concentration in very short time (Kime et al., 1996).

The acute, subacute and chronic toxicity studies of metals, nanomaterials, herbicides, pesticides and other toxic materials on fish and other aquatic living have been reported in a wide variety of ways. However, in recent years, several studies have been carried out to investigate of *in vitro* sperm toxicity of some toxic materials using CASA systems (Abascal, Cosson, & Fauvel, 2007; Chyb, Kime, Mikolajczyk, Szczerbik, & Epler, 2000; Chyb, Kime, Szczerbik, Mikolajczyk, & Epler, 2001; Dietrich et al., 2010; Fabbrocini et al., 2012; Kime et al., 1996; Li, Li, Dzyuba, & Randak, 2010; Van Look, & Kime, 2003). Recently, *in vitro* sperm toxicity will attract researcher's attention, thus, there are limited studies on toxicity of nanoparticles for risk assessment of nanomaterials.

ZnO NPs are widely used in several applications including cosmetics, plastic, paints, as drug carriers, UV-stabilizer, environmental remediation, wastewater treatment and fillings in medical materials (Dufour, Kumaravel, Nohynek, Kirkland, & Toutain, 2006; Vandebriel & De Jong, 2012). For Europe and the U.S., total concentration of ZnO NPs in surface waters was reported as 0.010 (0.008-0.055)  $\mu\text{g/l}$  and 0.001 (0.001-0.003)  $\mu\text{g/l}$ , respectively (Gottschalk, Sonderer, Scholz, & Nowack, 2009). The common carp (*Cyprinus carpio* L. 1758) is cultured fish for thousands of years and widely distributed throughout the world (Billard, Cosson, Percec, & Linhart, 1995). This fish species have lived in all fresh water such as a lake, river, dam and people have consumed both by catching and aquaculture. Therefore, we aimed to investigate the ecotoxicology of ZnO NPs which are participated to wetlands by direct or indirect, on especially proliferation of common carp. Besides all these, generally, it is known that ZnO NPs have toxic effects a wide range of organisms. But there are not many studies

describing the toxicity mechanism of ZnONPs on fish sperm and especially common carp sperm in the literature. So, in this study, it was evaluated the toxicological effect of flower-like ZnO NPs with different ratios (0.001, 0.01, 0.1, 0.5, 1 ppm) on spermatozoa motility of *Cyprinus carpio*. At the end of study, the motility parameters such as VSL ( $\mu\text{m/s}$ ), VCL ( $\mu\text{m/s}$ ), VAP ( $\mu\text{m/s}$ ), STR, BCF (Hz) and ALH ( $\mu\text{m}$ ), were recorded by CASA. [ÖME11]

## Materials and Methods

Zinc nitrate hexahydrate ( $\text{Zn}(\text{NO}_3)_2 \cdot 6\text{H}_2\text{O}$ ) was obtained from Merck, India. Potassium hydroxide (KOH) was purchased from Acros Organics. [E12] [13] *N*-methyl-2-pyrrolidone (NMP), pyridine, ethanol, tris(hydroxymethyl) aminomethane hydrochloride (Tris-HCl), sodium chloride (NaCl), potassium chloride (KCl) and potassium bromide (KBr) were purchased from Sigma-Aldrich. All the chemical reagents used in experiments were of analytical grade and used as received without further purification. All solutions used during the experiments were prepared using deionized water.

## Apparatus

The ZnO nanoparticles were firstly characterized by Fourier Transform Infrared Spectrometer (FTIR). Infrared spectrum of the prepared nanoparticles was recorded in the range  $4000 - 400 \text{ cm}^{-1}$ .

Thermal properties and thermal stability of the ZnO particles were performed with Shimadzu, differential thermal analysis (DTA) and thermogravimetric analysis (TGA). Initial sample was weighted as 10 mg for each operation. The sample was heated from  $\sim 24^\circ\text{C}$  to  $\sim 800^\circ\text{C}$  at the rate of  $10^\circ\text{C}/\text{min}$  in the air atmosphere.

The ZnO nanoparticles were characterized by X-ray diffraction (XRD) for the crystal structure and the impurity. Rigaku Rad B-Dmax II powder X-ray diffractometer was used for XRD patterns of these samples. The  $2\theta$  values were taken from  $15^\circ$  to  $80^\circ$  with a step size of  $0.04^\circ$  using Cu  $K\alpha$  radiation ( $\lambda$  value of  $2.2897\text{\AA}$ ).

The morphology of the obtained ZnO NPs was investigated by SEM (LEO Evo-40 VPX). Accelerating voltage was 2 kV, and the working distance was 3 mm for the analysis. In addition, the chemical composition of the ZnO NPs analyzed by EDAX; Röntech XFlash detector analyzer associated to a scanning electron microscope (SEM, Leo-Evo 40xVP). The beam was at normal incidence to the sample surface and the measurement time was 100 s. For the synthesis of nanoparticles with the flower-like morphology, the microwave oven was used. Microwave synthesis was carried out on a focused single-mode microwave synthesis system (2.45 GHz, Discover, CEM, USA). Microwave synthesis system was equipped with the magnetic stirring system and a water-cooled condenser outside the microwave cavity.

## Synthesis of Flower-Like ZnO NPs

0.297 g of  $\text{Zn}(\text{NO}_3)_2 \cdot 6\text{H}_2\text{O}$  (purity  $\geq 99.0\%$ ) and 5 mL of pyridine ( $\text{C}_5\text{H}_5\text{N}$ , purity  $\geq 99.5\%$ ) were dissolved in 50 mL of water. The solution was heated to  $90^\circ\text{C}$  in the microwave reactor to allow completion of the reaction for 10 minutes at this temperature. The product was collected by centrifugation and purified by washing several times with ethanol. Characterization was carried out by drying at  $60^\circ\text{C}$  and under vacuum. Then ZnO NPs were obtained and were stored room temperature for the experiments.

## Sperm Collection

*Cyprinus carpio* breeders were caught from the Karakaya reservoir on the Euphrates River in April, 2015 and the fishes were later transported to İnönü University Sürgü Fish Breeding Research Unit. The average weight of fishes was measured as  $157 \pm 12$  g. Here, after the adaptation period, direct sperm samples were taken from the fishes without hormone injection because of the breeding season.

### Preparation of Sperm Samples and Nanoparticle Exposure

Sperm samples were prepared using immotile and activation solutions reported by Poupard et al. (1998). Immotile solution (IMS) was adjusted with 30 mM Tris-HCl, pH 8.0, osmolality  $>390$  mosMkg<sup>-1</sup>, activation solution (AS) was adjusted with 45 mM NaCl, 5 mM KCl, 30 mM Tris-HCl, pH 8.0, osmolality  $<160$  mosMkg<sup>-1</sup>. Firstly, sperm samples were diluted at a ratio of 1:100 (1 sperm to 99 IMS) and then specified amounts of ZnO NPs (0.001, 0.01, 0.1, 0.5, 1 ppm) were added to eppendorf tube containing diluted sperm, respectively. All tubes were gently mixed and were incubated at 4°C for 4 hours. After the incubation period, each sperm sample was diluted with AS solution (1 sperm:20 AS) to examine motility analysis. Spermatozoa motility was evaluated using a light microscope (Olympus BX53, Tokyo, Japan) at 200× magnification with camera (Basler acA1300-30gc GigE). Also, video samples recorded at 30 fps frame rate. EC values were calculated on sperm motility parameters against different ZnO NPs doses by using GraphPad Prism 5 software.

### Processing of Images

Processing of sperm samples was carried out using the method described by (Pavlov, 2006) and Image J-Fiji program was used. To track of cell motility, it was used uncompressed AVI format videos, 8 bit >Threshold (Otsu) >MTrack2 plugin. The attained data were used to calculate the motility parameters (VSL, VCL, VAP, STR, BCF and ALH) values of the sperm cells in the application program (CASA.EXE), which was developed using the CASA.java plugin developed by (Wilson-Leedy & Ingermann, 2007).

### Statistical Analysis

Statistical analysis was performed using the program 'SPSS' for Windows (SPSS Inc., Chicago, IL, USA), version 17.0. Test of Homogeneity of Variances used to test the homogeneity and ANOVA test-Duncan Post-Hoc was also used for group comparisons via the GraphPad Prism 5 software (GraphPad Software, Inc., La Jolla, CA, USA). All values were expressed as means  $\pm$  SE. Any P value less than 0.05 were considered as statistically significant difference.

## Results

### Characterization of ZnO NPs

The composition and quality of the ZnO NPs were analyzed by the FTIR spectroscopy. The FTIR spectra of the flower-like ZnO NPs is presented in Figure 1. Metal oxides generally exhibit absorption bands in fingerprint region (i.e. below 1000 cm<sup>-1</sup>), which arise from inter-atomic vibrations. [E14] [I15] From spectra, the band at 523 cm<sup>-1</sup> is associated with stretching vibration of crystalline hexagonal ZnO. In addition to, the peak at 427 cm<sup>-1</sup> indicated conversion of Zn-O-Zn to ZnO. The peaks observed at ~3400 and 1630 cm<sup>-1</sup> are correlated to O-H stretching and assigned to adsorbed moisture in the sample, respectively. The absorption band at ~800 cm<sup>-1</sup> indicates the vibration of NO<sub>3</sub><sup>-</sup> ions, which may be due to zinc nitrate used in reaction. The peak at 1400-1450 cm<sup>-1</sup> is due to CO group

of carboxylic derivatives. Small absorption bands at  $\sim 900$  and  $2340\text{ cm}^{-1}$  associated with  $\text{CO}_2$  (C-O). The FTIR characterization of the structural and the chemical features of the flower-like ZnO NPs supports XRD results.

Figure 2 shows the X-ray diffraction pattern of flower-like ZnO NPs. All of the diffraction peaks can be indexed as the hexagonal ZnO phase (wurtzite-structure) by comparison with the data from JCPDS card files no. 36-1451. Peaks in the XRD pattern can be indexed to (100), (002), (101), (102), (110), (103), (200), (112), (201) and (202). The strong and narrow diffraction peaks indicate that the product has good crystallinity and large size. No characteristic peaks of other impurities such as  $\text{Zn}(\text{NO}_3)_2$  were detected in the diffractogram. The higher intensity of (002) peak compared to bulk ZnO indicated the growth orientation of ZnO nanorods towards C-axis. The XRD results indicated that the pure ZnO NPs were successfully synthesized.

The thermal properties of ZnO NPs were determined by DTA and TG. The TG curves (Figure 3) indicated the weight loss in two main temperature ranges,  $90^\circ\text{C}$  and  $350^\circ\text{C}$ . The first weight loss is at  $90^\circ\text{C}$ , which demonstrates the loss of surface-adsorbed water. The second main weight loss occurs in the  $350^\circ\text{C}$  ascribed to decomposing of ZnO. DTA curves of ZnO NPs were found to exhibit three exothermic peaks at  $250^\circ\text{C}$ ,  $250^\circ\text{C}$  and  $450^\circ\text{C}$  (Figure 3). The exothermic peaks at  $100^\circ\text{C}$  correspond to decomposition stage between  $90^\circ\text{C}$  and  $120^\circ\text{C}$  while the exothermic peak at  $250^\circ\text{C}$  corresponds to second decomposition stage ( $240^\circ\text{C}$  to  $260^\circ\text{C}$ ) in TGA (Figure 3).

The morphology of the synthesized ZnO NPs was characterized using SEM. Figures 4A, 4B, 4C and 4D show the representative SEM images of the ZnO NPs at different magnifications. It can be clearly observed that flower-like ZnO NPs are made of many hexagonal shaped nanorods.

Figure 5 shows the EDX and EDX-mapping spectrum of ZnO NPs. The strong peaks observed in the spectrum related to Zn and oxygen. It clearly confirms the presence of Zn and oxygen elements in the sample. Additionally, the EDX mapping images show the chemical composition of ZnO NPs (Figure 5). The Zn (red) ion and O (green) present together on the surface of ZnO NPs and the distribution of their composition is homogeneous. EDX and EDX mapping results confirmed that the prepared sample had very high purity.

### Sperm Motility Parameters

The average VSL value of the control group was measured as  $70.05 \pm 5.02\ \mu\text{m/s}$ . The changes of average VSL values of sperm samples exposed to different concentration ZnO NPs were no significant ( $P > 0.05$ ) (Figure 6a; Table 1).

The VCL value was the most affected parameter from ZnO NPs among the groups. While the average VCL value of control group was  $72.21 \pm 4.00\ \mu\text{m/s}$ , the velocity of sperm cells suddenly increased with the lowest dose of  $0.001\ \text{ppm}$  ZnO NPs. However, it was observed that the velocity remarkably reduced in with increasing ZnO NPs concentration. The maximum decline of velocity belongs to the  $1\ \text{ppm}$  ZnO NPs sample. Differences between the average VCL values were considered statistical significant ( $P < 0.05$ ) (Table 1, Figure 6b). In addition, EC50 of VCL value was calculated as  $0.56\ \text{ppm}$  (Figure 7).

The VAP values of sperm exposed to different concentration of ZnO NPs showed statistically significant ( $P < 0.05$ ) rely on concentration of ZnO NPs. The average VAP in the control group was  $64.17 \pm 2.26\ \mu\text{m/s}$ . Incubation of the sperm with ZnO NPs decreased to  $50.93 \pm 1.74$  at ZnO NPs concentrations of  $0.01\ \text{ppm}$  (Table 1, Figure 6c). Furthermore, the EC50 value of the VAP parameter was calculated  $0.004\ \text{ppm}$  (Figure 8).

Although the STR values of the spermatozoa were variable, the difference between the values was statistically insignificant ( $P > 0.05$ ). The lowest STR value is in the control group ( $1.10 \pm 0.09$ ), the highest STR value is in  $0.5$

ppm of ZnO NPs ( $1.40 \pm 0.07$ ) (Figure 6d). The values of BCF decreased in parallel with the concentration of ZnO NPs. There was statistically significant difference ( $P < 0.05$ ) between groups for BCF values (Figure 6e). The ALH values of spermatozoa decreased depending on ZnO concentrations, but this decrease was statistically insignificant ( $P > 0.05$ ) (Figure 6f, Table 1).

## Discussion

Microwave synthesis technique is an effective method for synthesizing nanosize materials because it is fast, clean and cost-effective, when compared with other methods. Conventional methods for zinc oxide synthesis require high temperatures and long reaction times. In recent years, one-dimensional ZnO nanostructures have been synthesized in the presence of catalysts using vapor phase synthesis. In addition to these studies, chemically and thermally stable ZnO nano structures have been obtained by hydrothermal methods and microemulsion methods. In this study, microwave method was used because of faster and economical synthesis.[E16] [IB17] The data obtained are in good agreement with other investigation results for ZnO NPs (Khan et al., 2016; Wu, Wu, & Lü, 2005; Ni et al., 2008; Bhat, 2008; Thambidurai, Muthukumarasamy, Velauthapillai, & Lee, 2013; Ahmad et al., 2011).

The goal of present study was to investigate the toxic impact of different concentration of ZnO NPs on sperm of *Cyprinus carpio* with the help of CASA. Recently, *in vitro* sperm toxicity will attract researcher's attention, thus, there are limited studies on toxicity of nanoparticles for risk assessment of nanomaterials. There are studies to determine *in vitro* sperm toxicity of some toxic substances using CASA systems in literature. For instance, Kime et al. (1996) investigated effects on the quality of fish sperm of some heavy materials using CASA systems. They revealed that the spermatozoa motility (VCL, VSL and VAP) of catfish (*Clarias gariepinus*) was affected after exposure to 100 ppm cadmium or 2000 ppm zinc in extender for 24 h. Yet, 1000 ppm cadmium or 2000 ppm zinc had any effect on motility when added to sperm at the final dilution stage.

In another study, the effects of Zn on spermatozoa motility of *Cyprinus carpio* were investigated by (Chyb, Kime, Mikolajczyk, Szczerbik, & Epler, 2000). The obtained results showed that there were statistically significant decreases in VSL, VCL and VAP values after 200 ppm and lethal concentration was 500 ppm. In addition to, the same authors reported that mercury (Hg) decreased the time of spermatozoa movement at doses as low as 0.2 ppm, and that lethal effects were evident at 0.5 and 1 ppm (Chyb, Sokolowska, Kime, Socha, & Epler, 2001).[E18] In [ÖME19] similar work cadmium (Cd) decreases the motility of carp spermatozoa in all tested concentrations, and that lethal effect was calculated 500 ppm by CASA (Chyb, Kime, Szczerbik, Mikolajczyk, & Epler, 2001). Investigated the effects of Hg on sperms of goldfish (*Carassius auratus*) and discussed parameters of spermatozoa motility in terms of VCL value and spermatozoa morphology. According to the study, they found that concentrations of 1-10 mg/l mercury chloride ( $\text{HgCl}_2$ ) significantly reduced VCL value of sperms and 100 mg/l of  $\text{HgCl}_2$  shortened the flagellum length of spermatozoa (Van Look & Kime, 2003).

The effects of lead chloride ( $\text{PbCl}_2$ ), copper chloride ( $\text{CuCl}_2 \cdot 2\text{H}_2\text{O}$ ) and  $\text{HgCl}_2$  on the sperm of sea bass (*Dicentrarchus labrax*) were investigated by adding 0.01, 0.1, 1, 10 and 100 ppm ratios to the activation solution. In study, since spermatozoa motility of sea bass is very short (<50s), all of spermatozoa motility parameters declined at the first 20 s. Moreover, it was observed that  $\text{Cu}^{2+}$  and  $\text{Pb}^{2+}$  did not affect spermatozoa motility when the activation solution contained up to 100 ppm of the metal salts. However, 0.4–1 ppm (sperm dilution rate 1:39) of  $\text{HgCl}_2$  changed the morphology of post-swimming spermatozoas and their motility completely arrested at



concentrations as low as 0.1 ppm (sperm dilution rate 1:2500) of  $\text{HgCl}_2$  (Abascal, Cosson, & Fauvel, 2007). The modified sperms of rainbow trout using Hg (1-10 mg/l) and Cd (10 mg/l) and reported changes in their spermatozoa motility after 4 h incubation (Dietrich et al., 2010). Similarly, Li, Li, Dzyuba, & Randak (2010) investigated the motility parameters and antioxidant effect on sperm of Sterlet (*Acipenser ruthenus*) of heavy metals. They examined effect of heavy metals (Cd, Cr and Cd+Cr) for 2 h incubation. Results revealed that the concentrations (5 mg/l Cr, 0.05 mg/l Cd and 5 mg/l Cr + 0.05 mg/l Cd) inhibited motility parameters. The ecotoxicological effects of Cd were studied on the storage of sperm of the *Sparus aurata* (Fabbrocini et al., 2012). The authors found that 50 mg/l of Cd had insignificant differences on spermatozoa motility compared to the control group.

In the present study, following 4 h incubation, the average VSL values showed a gradual decrease and a decreasing-increasing velocity. Besides, statistical significance was defined as  $P > 0.05$  for VSL (Figure 1a). A similar result has been observed in study of (Li, Li, Dzyuba, & Randak, 2010) which investigated the effects of Cd and Cr on sperm of Sterlet (*Acipenser ruthenus*).

In our study, it was observed that the value of VCL significantly decreased in parallel with concentration of ZnO NPs. According to VCL values, 0.5 ppm of ZnO NPs exerted a lethal effect on sperm cells and the difference was statistically significant ( $P < 0.05$ ) (Figure 1b). The same phenomenon was observed in VAP values and these values started to decrease with concentration of 0.01 ppm (Figure 1c). The obtained results are consistent with the literature and similar results were reported by (Kime et al., 1996; Chyb, Mikolajczyk, Szczerbik, & Epler, 2000; Dietrich et al., 2010). [E20] [ÖME21]

In teleost fish, spermatozoa generally move along a straight or slightly curved immediately after activation. Spermatozoa motion orbits may increase its curve during exposure to contaminants, or in the non-conforming diluents towards the end of the activation period, and the circles in the interior may turn into shapes. Under these conditions, linearity (LIN, the ratio of net distance moved to total path distance (VSL/VCL)) or straightness (STR, the ratio of net distance moved to smoothed path distance (VSL/VAP)) may be very important parameters to detect of curvature of the orbit. Fertilization can depend on both the number of motile spermatozoa and their speed (Rurangwa, Kime, Ollevier, & Nash, 2004). In this study, as the concentration of ZnO NPs increased, the value of STR increased. This implies an increase in properties of curved orbit in the movements of spermatozoa exposed to ZnO NPs. Thus, the fertilization ability of spermatozoa movements reduced. According to the obtained results, there was statistically significant difference ( $P < 0.05$ ) for BCF in parallel with the concentration of ZnO NPs. In the ALH values, the differences were not significant ( $P > 0.05$ ) compared with the control group. Besides, BCF values are different from (Fabbrocini et al., 2012), but ALH values showed parallelism. [E22]

[ÖME23]

## Conclusion

In this study, flower-like ZnO NPs were synthesized via microwave-assisted solvothermal techniques and were characterized using structural, thermal and morphological techniques. The ecotoxicological effects of ZnO NPs (0.001, 0.01, 0.1, 0.5, and 1 ppm) on the motility and acceleration properties of *Cyprinus carpio* sperm samples were determined with CASA system as *in vitro*. Especially, VCL, VAP and BCF values were significantly affected by ZnO NP-treatment. On the basis of these experiments, the EC50 values of VCL and VAP parameters were calculated 0.56 ppm and 0.004 ppm, respectively. Consequently, the finding of this study support that fish spermatozoa is an important indicator in ecotoxicology studies and will be helpful in determining the toxic doses of ZnO NPs.

**References**[E24][ÖME25]

- Abascal, F. J., Cosson, J., & Fauvel, C. (2007). Characterization of sperm motility in sea bass: The effect of heavy metals and physicochemical variables on sperm motility. *Journal of Fish Biology*, 70(2), 509–522. <https://doi.org/10.1111/j.1095-8649.2007.01322.x>
- Ahmad, M., Yingying, S., Nisar, A., Sun, H., Shen, W., Wei, M., & Zhu, J. (2011). Synthesis of hierarchical flower-like ZnO nanostructures and their functionalization by Au nanoparticles for improved photocatalytic and high performance Li-ion battery anodes. *Journal of Materials Chemistry*, 21 (December 2015), 7723. <https://doi.org/10.1039/c1jm10720h>
- Alavi, S. M. H., & Cosson, J. (2005). Sperm motility in fishes. I. Effects of temperature and pH: A review. *Cell Biology International*, <https://doi.org/10.1016/j.cellbi.2004.11.021>
- Alavi, S. M. H., Hatef, A., Psenicka, M., Kaspar, V., Boryshpolets, S., Dzyuba, B., ... Linhart, O. (2012). Sperm biology and control of reproduction in sturgeon: (II) sperm morphology, acrosome reaction, motility and cryopreservation. *Reviews in Fish Biology and Fisheries*, <https://doi.org/10.1007/s11160-012-9270-x>
- Bhat, D. K. (2008). Facile synthesis of ZnO nanorods by microwave irradiation of zinc-hydrazine hydrate complex. *Nanoscale Research Letters*, 3(1), 31–35. <https://doi.org/10.1007/s11671-007-9110-4>
- Billard, R., Cosson, J., Perchec, G., & Linhart, O. (1995). Biology of sperm and artificial reproduction in carp. *Aquaculture*, 129(1–4), 95–112. [https://doi.org/10.1016/0044-8486\(94\)00231-C](https://doi.org/10.1016/0044-8486(94)00231-C)
- Chyb, J., Kime, D. E., Mikolajczyk, T., Szczerbik, P., & Epler, P. (2000). The influence of zinc on sperm motility of common carp—a computer assisted studies. *Archiwum Rybactwa*, 8(1974), 5–14.
- Chyb, J., Kime, D. E., Szczerbik, P., Mikolajczyk, T., & Epler, P. (2001). Computer assisted analysis (CASA) of common carp *Cyprinus carpio* L. spermatozoa motility in the presence of cadmium. *Archives of Polish Fisheries*, 9(2), 173–181.
- Chyb, J., Sokolowska, M., Kime, D.E., Socha, M., & Epler, P. (2001). The influence of mercury on computer analyzed sperm motility of common carp, *Cyprinus carpio* L., in vitro. *Archives of Polish Fisheries*, 9(1), 51–60.
- Coward, K., Bromage, N. R., Hibbitt, O., & Parrington, J. (2002). Gamete physiology, fertilization and egg activation in teleost fish. *Reviews in Fish Biology and Fisheries*, 12(1), 33–58. <https://doi.org/10.1023/A:1022613404123>
- Dietrich, G. J., Dietrich, M., Kowalski, R. K., Dobosz, S., Karol, H., Demianowicz, W., & Glogowski, J. (2010). Exposure of rainbow trout milt to mercury and cadmium alters sperm motility parameters and reproductive success. *Aquatic Toxicology*, 97(4), 277–284. <https://doi.org/10.1016/j.aquatox.2009.12.010>
- Dufour, E. K., Kumaravel, T., Nohynek, G. J., Kirkland, D., & Toutain, H. (2006). Clastogenicity, photo-clastogenicity or pseudo-photo-clastogenicity: Genotoxic effects of zinc oxide in the dark, in pre-irradiated or simultaneously irradiated Chinese hamster ovary cells. *Mutation Research - Genetic Toxicology and Environmental Mutagenesis*, 607(2), 215–224. <https://doi.org/10.1016/j.mrgentox.2006.04.015>
- Fabbrocini, A., D'Adamo, R., Del Prete, F., Luca Langellotti, A., Rinna, F., Silvestri, F., ... Sansone, G. (2012). Cryopreserved semen in ecotoxicological bioassays: Sensitivity and reliability of cryopreserved *Sparus aurata* spermatozoa. *Ecotoxicology and Environmental Safety*, 84, 293–298. <https://doi.org/10.1016/j.ecoenv.2012.07.024>
- Gottschalk, F., Sonderer, T., Scholz, R. W., & Nowack, B. (2009). Modeled environmental concentrations of engineered nanomaterials (TiO<sub>2</sub>, ZnO, Ag, CNT, fullerenes) for different regions. *Environmental Science and Technology*, 43(24), 9216–9222. <https://doi.org/10.1021/es9015553>
- Hatef, A., Alavi, S. M. H., Golshan, M., & Linhart, O. (2013). Toxicity of environmental contaminants to fish spermatozoa function in vitro—A review. *Aquatic Toxicology*, <https://doi.org/10.1016/j.aquatox.2013.05.016>
- Khan, M.F., Ansari, A.H., Hameedullah, M., Ahmad, E., Husain, F.M., Zia, Q., Baig, U., ... Aliev, G., (2016). Sol-gel synthesis of thorn-like ZnO nanoparticles endorsing mechanical stirring effect and their antimicrobial activities: Potential role as nano-antibiotics. *Scientific Reports*, 6 (27689), 1-12. <https://doi.org/10.1038/srep27689>
- Kime, D. E., Ebrahimi, M., Nysten, K., Roelants, I., Rurangwa, E., Moore, H. D. M., & Ollevier, F. (1996). Use of computer assisted sperm analysis (CASA) for monitoring the effects of pollution on sperm quality of fish; application to the effects of heavy metals. *Aquatic Toxicology*, 36(3–4), 223–237. [https://doi.org/10.1016/S0166-445X\(96\)00806-5](https://doi.org/10.1016/S0166-445X(96)00806-5)
- Li, Z. H., Li, P., Dzyuba, B., & Randak, T. (2010). Influence of environmental related concentrations of heavy metals on motility parameters and antioxidant responses in sturgeon sperm. *Chemico-Biological Interactions*, 188(3), 473–477. <https://doi.org/10.1016/j.cbi.2010.09.005>
- Ni, Y., Wu, G., Zhang, X., Cao, X., Hu, G., Tao, A., Yang, Z., & Wei, X. (2008). Hydrothermal preparation, characterization and property research of flowerlike ZnO nanocrystals built up by nanoflakes. *Materials Research Bulletin*, 43(11), 2919–2928. <https://doi.org/10.1016/j.materresbull.2007.12.004>
- Pavlov, D. A. (2006). A method for the assessment of sperm quality in fish. *Journal of Ichthyology*, 46(5), 391–398. <https://doi.org/10.1134/S0032945206050055>
- Poupard, G. P., Paxion, C., Cosson, J., Jeulin, C., Fierville, F., & Billard, R. (1998). Initiation of carp spermatozoa motility and early ATP reduction after milt contamination by urine. *Aquaculture*, 160, 317–328. [https://doi.org/10.1016/S0044-8486\(97\)00301-3](https://doi.org/10.1016/S0044-8486(97)00301-3)
- Rurangwa, E., Kime, D. E., Ollevier, F., & Nash, J. P. (2004). The measurement of sperm motility and factors affecting sperm quality in cultured fish. *Aquaculture*, 234(1–4), 1-28. <https://doi.org/10.1016/j.aquaculture.2003.12.006>
- Thambidurai, M., Muthukumarasamy, N., Velauthapillai, D., & Lee, C. (2013). Synthesis and characterization of flower like ZnO nanorods for dye-sensitized solar cells. *Journal of Materials Science: Materials in Electronics*, 24(7), 2367–2371. <https://doi.org/10.1007/s10854-013-1103-8>
- Van Look, K. J. W., & Kime, D. E. (2003). Automated sperm morphology analysis in fishes: The effect of mercury on goldfish



- sperm. *Journal of Fish Biology*, 63(4), 1020–1033. <https://doi.org/10.1046/j.1095-8649.2003.00226.x>
- Vandebriel, R. J., & De Jong, W. H. (2012). A review of mammalian toxicity of ZnO nanoparticles. *Nanotechnology, Science and Applications*, <https://doi.org/10.2147/NSA.S23932>
- Wilson-Leedy, J. G., & Ingermann, R. L. (2007). Development of a novel CASA system based on open source software for characterization of zebrafish sperm motility parameters. *Theriogenology*, 67(3), 661–672. <https://doi.org/10.1016/j.theriogenology.2006.10.003>
- Wu, L., Wu, Y., & Lü, W. (2005). Preparation of ZnO Nanorods and optical characterizations. *Physica E: Low-Dimensional Systems and Nanostructures*, 28(1), 76–82. <https://doi.org/10.1016/j.physe.2005.02.005>

**Table 1.** Descriptive results of motility parameters after exposed ZnO NP.

	N=5	Mean±Std. Error	95% Confidence Interval for Mean		Sig. *(P<0.05)
			Lower Bound	Upper Bound	
VSL: Straight Line Velocity (µm/s)	Control	70.05±5.02	56.12	83.98	0.85
	0.001 ppm	74.54±4.29	62.63	86.46	
	0.01 ppm	66.91±6.58	48.63	85.19	
	0.1 ppm	65.98±2.34	59.50	72.46	
	0.5 ppm	71.64±2.45	64.83	78.44	
	1 ppm	69.70±7.21	49.68	89.72	
VCL: Higher Curvilinear Velocity (µm/s)	Control	72.21±4.00 <sup>c</sup>	61.11	83.31	0.00*
	0.001 ppm	118.50±5.76 <sup>a</sup>	102.51	134.49	
	0.01 ppm	99.62±6.90 <sup>b</sup>	80.47	118.77	
	0.1 ppm	87.54±3.88 <sup>b</sup>	76.75	98.33	
	0.5 ppm	65.61±5.55 <sup>c</sup>	50.20	81.02	
	1 ppm	26.14±2.70 <sup>d</sup>	18.63	33.64	
VAP: Average Path Velocity (µm/s)	Control	64.17±2.26 <sup>a</sup>	57.88	70.45	0.00*
	0.001 ppm	65.08±0.38 <sup>a</sup>	64.01	66.15	
	0.01 ppm	51.48±1.58 <sup>b</sup>	47.08	55.88	
	0.1 ppm	50.93±1.74 <sup>b</sup>	46.10	55.77	
	0.5 ppm	51.36±1.77 <sup>b</sup>	46.44	56.28	
	1 ppm	52.53±0.70 <sup>b</sup>	50.58	54.48	
STR: Straightness of Average Route (VSL/VAP)	Control	1.10±0.09	0.85	1.35	0.29
	0.001 ppm	1.15±0.07	0.95	1.34	
	0.01 ppm	1.32±0.15	0.89	1.74	
	0.1 ppm	1.30±0.04	1.17	1.42	
	0.5 ppm	1.40±0.07	1.22	1.59	
	1 ppm	1.33±0.14	0.94	1.72	
BCF: Beat Cross Frequency (cross/second) (Hz)	Control	1.78±0.14 <sup>a</sup>	1.41	2.16	0.03*
	0.001 ppm	1.78±0.24 <sup>a</sup>	1.13	2.44	
	0.01 ppm	1.59±0.19 <sup>ab</sup>	1.06	2.11	
	0.1 ppm	1.28±0.15 <sup>ab</sup>	0.86	1.70	
	0.5 ppm	1.16±0.10 <sup>b</sup>	0.88	1.45	
	1 ppm	1.17±0.16 <sup>b</sup>	0.72	1.61	
ALH: Amplitude of Lateral Displacement of the Sperm Head (µm)	Control	17.76±1.25	14.29	21.23	0.86
	0.001 ppm	17.09±2.32	10.64	23.53	
	0.01 ppm	14.07±2.95	5.88	22.26	
	0.1 ppm	16.40±1.91	11.10	21.70	
	0.5 ppm	15.01±2.11	9.16	20.86	
	1 ppm	15.88±2.36	9.33	22.42	

Significant differences (P <0.05) were showed in the values indicated by different superscripted letters according to one-way ANOVA with Duncan's multiple range test.

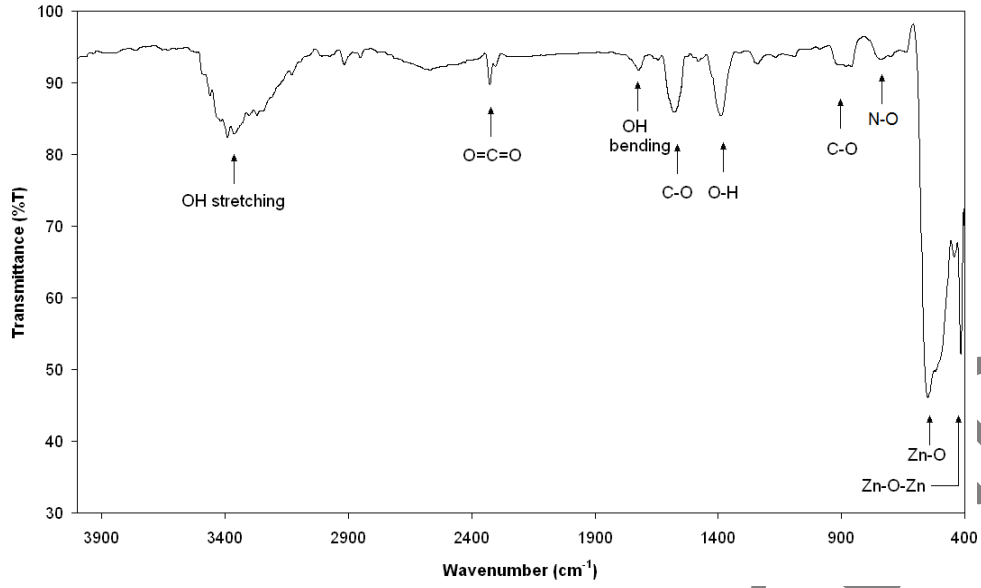


Figure 1. FTIR spectra of flower-like ZnO NPs.

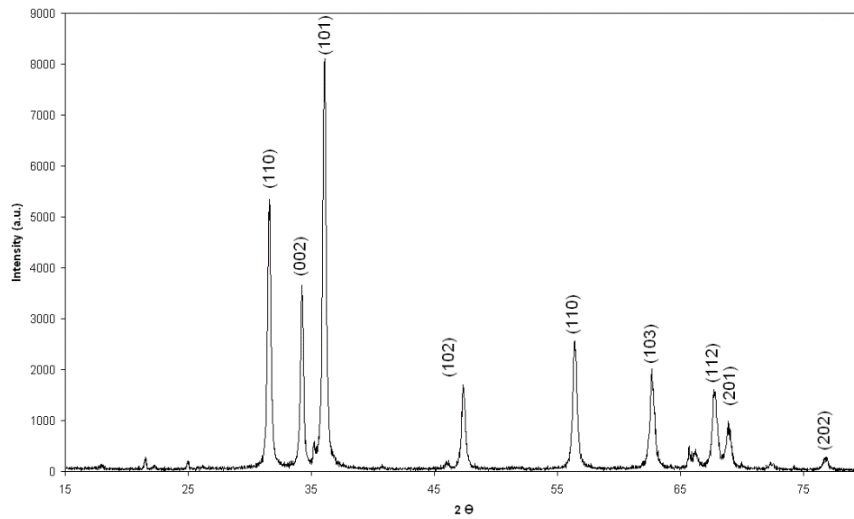


Figure 2. XRD patterns of flower-like ZnO NPs

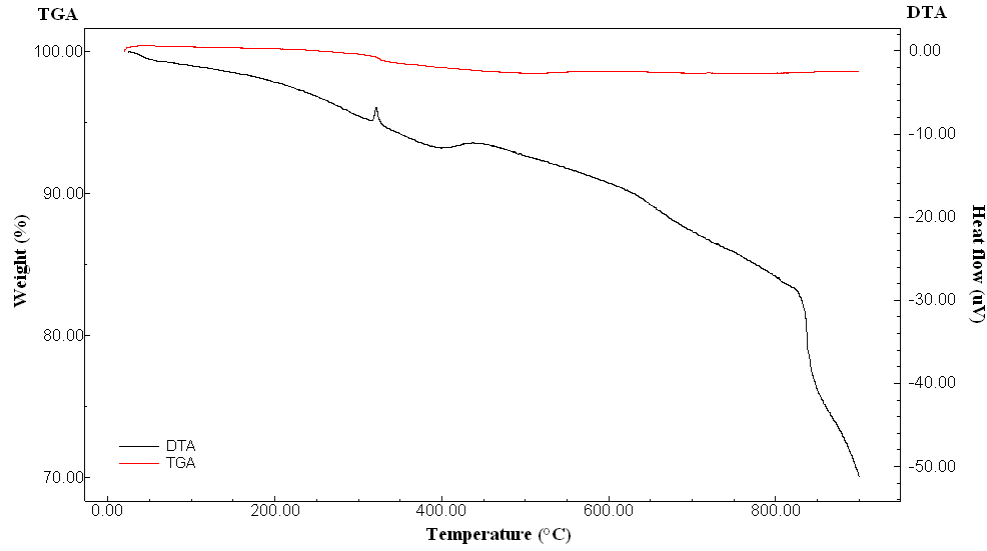


Figure 3. TG thermogram and DTA thermogram of ZnO NPs

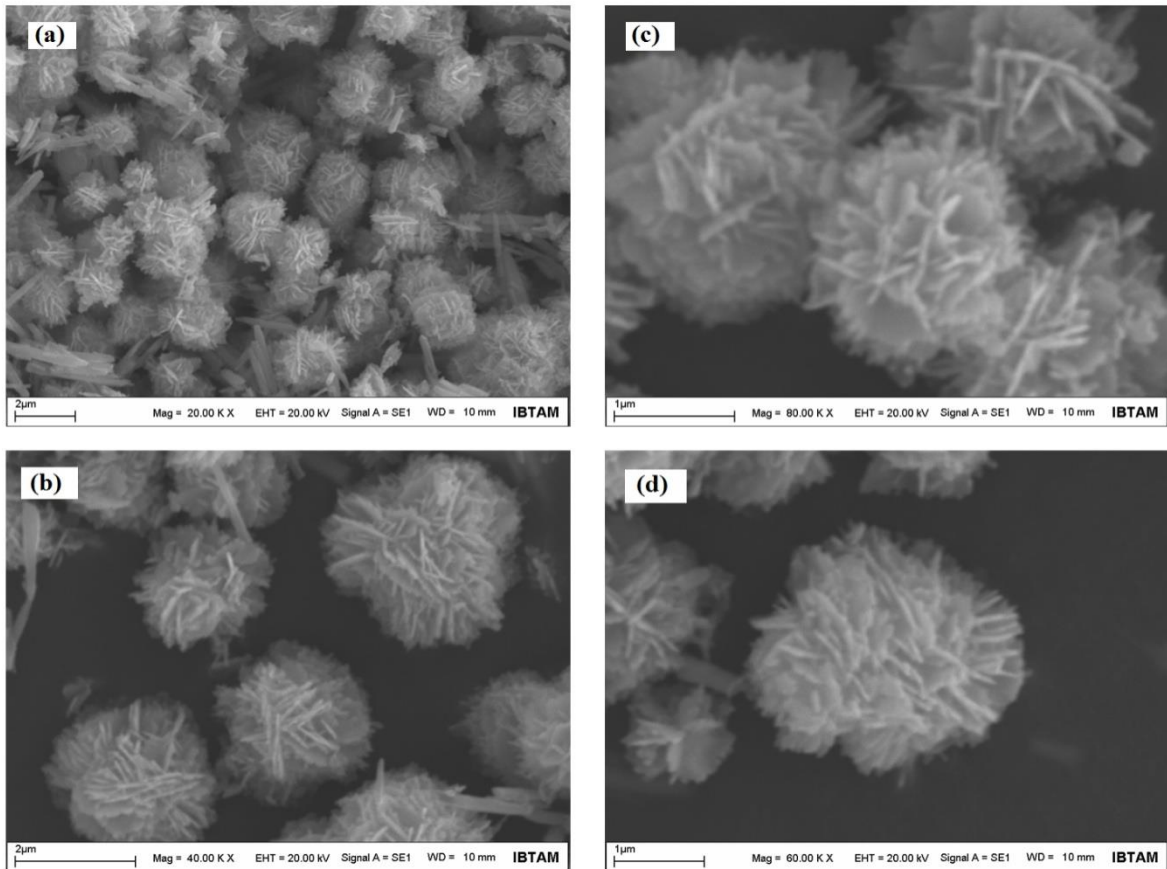


Figure 4. High (a,b) and low (c,d) magnification SEM images of flower-like ZnO NPs.

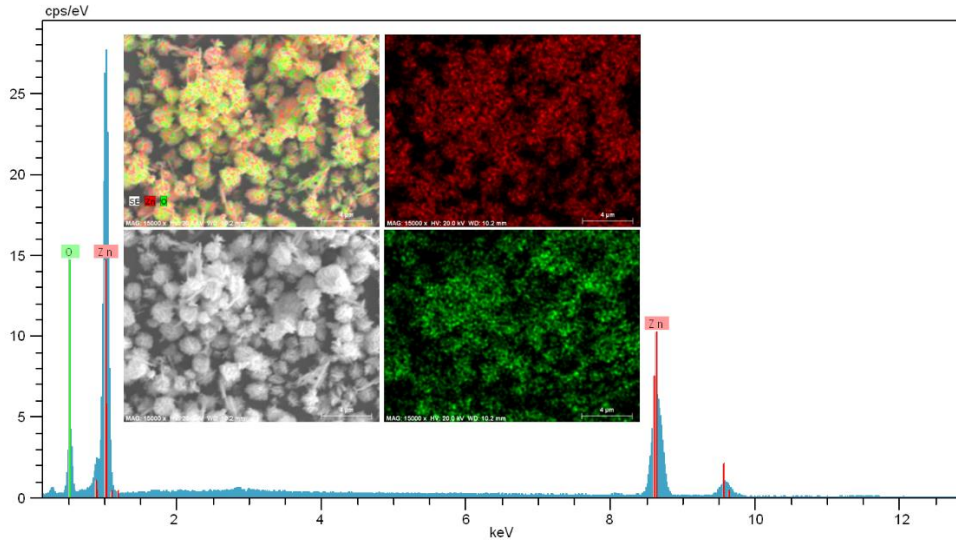


Figure 5. EDX images of flower-like ZnO NPs.

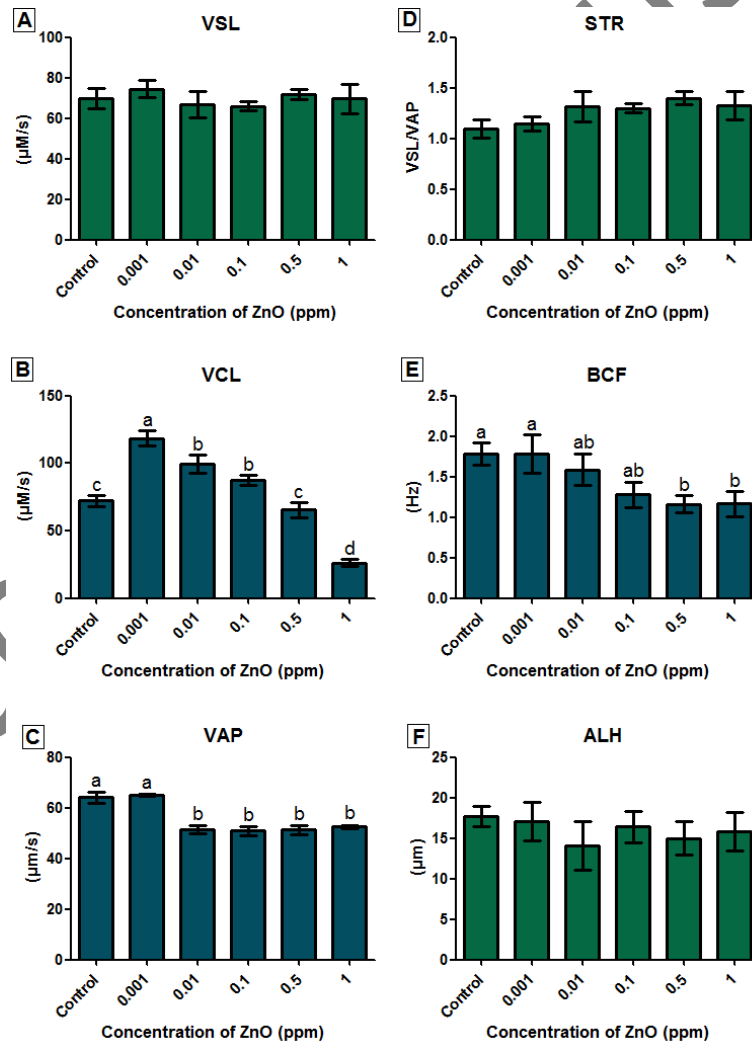


Figure 6. The effects of different ZnO NP concentrations on straight line velocity (VSL), curvilinear velocity (VCL), average path velocity (VAP), straightness (STR), beat cross frequency (BCF), amplitude of lateral displacement of the sperm head (ALH) in common carp sperm. A represents VSL, B represents VCL, C represents VAP, D represents STR, E represents BCF and F represents ALH. The different letters reflect statistically different values ( $P < 0.05$ ).

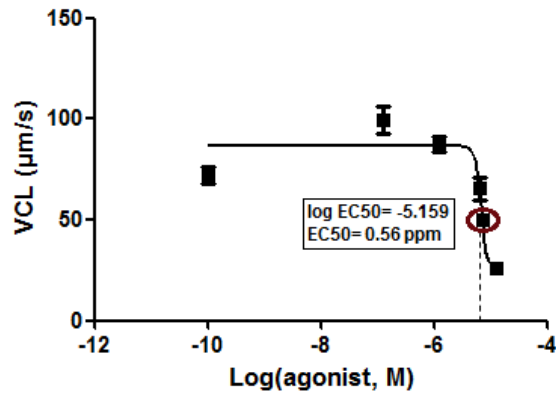


Figure 7. Effective concentration( $EC_{50}$ ) of ZnO NPs on curvilinear velocity (VCL)

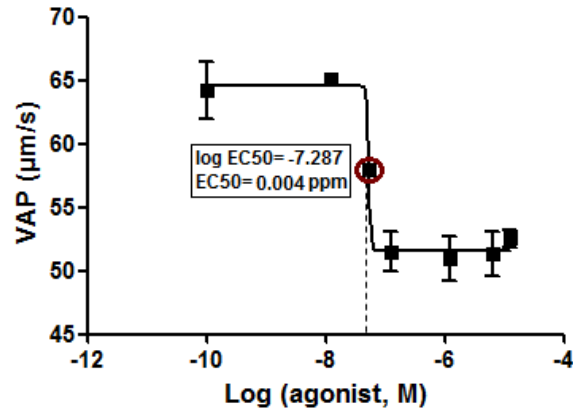


Figure 8. Effective concentration( $EC_{50}$ ) of ZnO NPs on average path velocity (VAP)